ARTICLE

Discovery and Validation of Novel Expression Signature for Postcystectomy Recurrence in High-Risk Bladder Cancer

Anirban P. Mitra, Lucia L. Lam, Mercedeh Ghadessi, Nicholas Erho, Ismael A. Vergara, Mohammed Alshalalfa, Christine Buerki, Zaid Haddad, Thomas Sierocinski, Timothy J. Triche, Eila C. Skinner, Elai Davicioni, Siamak Daneshmand*, Peter C. Black*

*Authors contributed equally to this work.

Manuscript received February 4, 2014; revised June 4, 2014; accepted August 8, 2014.

Correspondence to: Anirban P. Mitra, MD, PhD, Department of Pathology and Center for Personalized Medicine, University of Southern California, 4650 Sunset Boulevard, MS 103, Los Angeles, CA 90027 (e-mail: apmitra@gmail.com).

Background	Nearly half of muscle-invasive bladder cancer patients succumb to their disease following cystectomy. Selecting candidates for adjuvant therapy is currently based on clinical parameters with limited predictive power. This study aimed to develop and validate genomic-based signatures that can better identify patients at risk for recurrence than clinical models alone.
Methods	Transcriptome-wide expression profiles were generated using 1.4 million feature-arrays on archival tumors from 225 patients who underwent radical cystectomy and had muscle-invasive and/or node-positive bladder cancer. Genomic (GC) and clinical (CC) classifiers for predicting recurrence were developed on a discovery set (n = 133). Performances of GC, CC, an independent clinical nomogram (IBCNC), and genomic-clinicopathologic classifiers (G-CC, G-IBCNC) were assessed in the discovery and independent validation (n = 66) sets. GC was further validated on four external datasets (n = 341). Discrimination and prognostic abilities of classifiers were compared using area under receiver-operating characteristic curves (AUCs). All statistical tests were two-sided.
Results	A 15-feature GC was developed on the discovery set with area under curve (AUC) of 0.77 in the validation set. This was higher than individual clinical variables, IBCNC (AUC = 0.73), and comparable to CC (AUC = 0.78). Performance was improved upon combining GC with clinical nomograms (G-IBCNC, AUC = 0.82; G-CC, AUC = 0.86). G-CC high-risk patients had elevated recurrence probabilities ($P < .001$), with GC being the best predictor by multivariable analysis ($P = .005$). Genomic-clinicopathologic classifiers outperformed clinical nomograms by decision curve and reclassification analyses. GC performed the best in validation compared with seven prior signatures. GC markers remained prognostic across four independent datasets.
Conclusions	The validated genomic-based classifiers outperform clinical models for predicting postcystectomy bladder cancer recurrence. This may be used to better identify patients who need more aggressive management.

Of the 386,300 urinary bladder cancer cases diagnosed annually worldwide, nearly 30% present with disease invading the muscle layer of the bladder (1). Although radical cystectomy can improve cancer-specific outcomes, long-term prognosis continues to be compromised by the high risk for recurrence, which occurs in 40% to 50% of patients (2,3). Postcystectomy recurrence of urothelial carcinoma of the bladder (UCB) is ultimately fatal in 85% to 95% of patients (4,5).

Contemporary adjuvant chemotherapy shows modest success in delaying or preventing UCB recurrence and is associated with substantial toxicity (6). Identification of candidates at high risk for recurrence who may benefit most from adjuvant chemotherapy is currently based on standard clinicopathologic criteria (7). Even when combined as multivariable nomograms, these metrics do not fully account for the diverse clinical behavior of muscle-invasive

UCB (8,9). It is now recognized that biomarker panels that reflect the biological heterogeneity of UCB can better identify patients who need aggressive therapy than single molecular markers alone (10,11). Unbiased and pathway-specific approaches have been previously used to identify prognostic molecular signatures in UCB (12–19). However, such panels have not been implemented clinically because of several shortcomings: signature development on underpowered and clinically heterogeneous cohorts thereby potentially resulting in data overfitting, short follow-up and use of non-disease-specific endpoints, reliance on fresh tumor tissues, and limited validation.

To address the clinical need for accurate and reproducible identification of patients with aggressive disease postcystectomy, we performed unbiased transcriptome-wide expression profiling on a cohort of uniformly-treated patients with muscle-invasive and/

or pathologically node-positive (hereafter referred to as clinically high-risk) UCB, the largest such effort in this disease stage to date. This resulted in the discovery of a 15-marker genomic signature that robustly identifies patients at greatest risk for recurrence. The performance of this signature was improved by addition of clinicopathologic variables. The prognostic potential of the locked signature was confirmed by blinded independent validation, and was shown to outperform previously reported gene signatures.

Methods

Patient Population and Specimen Processing

The study cohort was composed of 225 patients with organ-confined, muscle-invasive (pT2N0M0), extravesical (pT3-4aN0M0), and node-positive (pTanyN1-3M0) UCB who underwent radical cystectomy at the University of Southern California between 1998 and 2004 (2). Each patient had a minimum two-year follow-up postcystectomy unless they recurred prior to that date. Patients receiving neoadjuvant chemotherapy, and those with clinical evidence of lymphadenopathy or distant metastasis at diagnosis were excluded. Patients underwent extended pelvic lymphadenectomy and urinary diversion. Tumor staging was standardized to American Joint Committee on Cancer recommendations (20). Ninety-eight (43.6%) patients received adjuvant chemotherapy per physician and patient preference. Postoperative follow-up was at four-month intervals in year one, six-month intervals in year two, and annually thereafter (4).

With bioinformaticians who generated the prognostic classifiers remaining blinded to clinical data, two-thirds of the cohort was assigned to a discovery set and one-third to a validation set, with clinicopathologic characteristics balanced between both sets. Clinical endpoint for biomarker discovery was cancer recurrence. Recurrence-free survival (RFS) duration was defined as time from cystectomy to cancer recurrence at local or distant soft tissue sites; patients who were recurrence-free at end of the study were censored at death or last follow-up. De novo urothelial carcinoma in upper tract or urethra was not considered as recurrence. RFS was preferred as the endpoint over cancer-specific survival because most patients who die of UCB have documentation of disease recurrence (3); this also avoided censoring patients with aggressive disease who recurred but died of other comorbidities.

Formalin-fixed paraffin-embedded (FFPE) primary tumor specimens underwent histopathological rereview, RNA extraction and profiling using GeneChip Human Exon 1.0 ST microarrays (Affymetrix, Santa Clara, CA). These arrays profile coding and noncoding regions of the entire human transcriptome using probe selection regions, hereinafter referred to as features. Specimen and microarray processing are detailed in the Supplementary Methods (available online). Samples from 199 (88.4%) patients passed microarray quality control; relative patient proportions in discovery (n = 133) and validation (n = 66) sets were maintained (Table 1). The University of Southern California Institutional Review Board approved this study and all patients consented to analysis of their tumor tissues.

Classifier Development and Application

Features most predictive of RFS were identified and combined as a signature to produce a genomic classifier (GC) (see the Supplementary Methods, available online). Prognostic ability of GC was benchmarked against two clinical nomograms for predicting postcystectomy recurrence risk: the International Bladder Cancer Nomogram Consortium (IBCNC) (8), and an in-house "clinical-only" classifier (CC). The latter incorporated age, gender, pathological stage, and lymphovascular invasion status into a logistic regression model. Additionally, to evaluate the joint prognostic value of genomic and clinicopathologic variables, GC was integrated with IBCNC and CC into G-IBCNC and G-CC, respectively (collectively referred to as genomic-clinicopathologic classifiers) by logistic regression. All classifiers output a continuous score between 0 and 1, with higher scores indicating higher probability of recurrence. Locked classifiers were then applied to the validation set in a blinded fashion. Supplementary Figure 1 (available online) provides an overview of the study design.

GC performance was compared with prior prognostic genomic signatures for muscle-invasive or node-positive UCB (13-15,21,22). Prognostic ability of GC was also independently validated on four external UCB datasets (see the Supplementary Methods, available online).

Statistical and Biological Analyses

Discrimination and prognostic abilities of classifiers were compared using area under receiver-operating characteristic (ROC) curves (AUCs) for binary and time-to-event outcomes, and other methods. Cumulative incidence curves for RFS were constructed using Fine-Gray competing risk analyses (23). Decision curve and reclassification analyses were used to determine the clinical value of classifiers. Where categorized, classifier scores of greater than or equal to 0.5 and less than 0.5 were grouped as high-risk and low-risk, respectively.

Biological interactions of GC components with their first-degree partners were extracted using Human Signaling Network v5 (24–27). Processes were grouped using Enrichment Map, with nodes and links representing Gene Ontology (GO) terms and degree of overlap between them, respectively (28). Analyses are further detailed in the Supplementary Methods (available online).

Results

Discovery and Initial Performance of Genomic-Based Classifiers

To test the hypothesis that risk-prediction models incorporating genomic signatures can better characterize the biology that determines propensity of UCB to recur postcystectomy than clinical variables alone, a genomic classifier (GC) was developed and tested on the discovery set. Patient characteristics are listed in Table 1. Median age was 68.5 years (interquartile range [IQR] = 63.6–75.6). Median follow-up was 9.3 years; 68 (51.1%) patients recurred, and 77 (57.9%) patients were dead at last follow-up.

Expression of nearly 1.4×10^6 RNA features in tumors of patients who recurred was compared with those who remained recurrence-free at last follow-up (Supplementary Figure 2, available online). Following normalization and feature selection, 15 markers were identified corresponding to RNAs from protein-coding and noncoding regions of the genome that were differentially expressed based on recurrence (Supplementary Table 1, available online). A random forest machine-learning algorithm assembled

Table 1. Clinicopathologic characteristics of patients in the discovery and validation sets*

Characteristic	Discovery set				Validation set				Discovery vs validation
	Total n (set %)	Not recurred n (column %)†	Recurred n (column %)†	Not recurred vs recurred P	Total n (set %)	Not recurred n (column %)†	Recurred n (column %)†	Not recurred vs recurred P	P
Total (row %)	133 (100)	65 (48.9)	68 (51.1)		66 (100)	33 (50.0)	33 (50.0)		
Age				.49				1.00	.55
<70 years	73 (54.9)	38 (58.5)	35 (51.5)		33 (50.0)	17 (51.5)	16 (48.5)		
≥70 years	60 (45.1)	27 (41.5)	33 (48.5)		33 (50.0)	16 (48.5)	17 (51.5)		
Sex				.82				.73	1.00
Male	111 (83.5)	55 (84.6)	56 (82.4)		56 (84.8)	29 (87.9)	27 (81.8)		
Female	22 (16.5)	10 (15.4)	12 (17.6)		10 (15.2)	4 (12.1)	6 (18.2)		
Race				.32				.43	.65
Caucasian	115 (86.5)	54 (83.1)	61 (89.7)		59 (89.4)	31 (93.9)	28 (84.8)		
Non-Caucasian	18 (13.5)	11 (16.9)	7 (10.3)		7 (10.6)	2 (6.1)	5 (15.2)		
Tumor stage				.033				.013	.76
pT1	3 (2.3)	1 (1.5)	2 (3.0)		3 (4.5)	2 (6.1)	1 (3.0)		
pT2	44 (33.1)	28 (43.1)	16 (23.5)		20 (30.3)	13 (39.4)	7 (21.2)		
pT3	58 (43.6)	28 (43.1)	30 (44.1)		31 (47.0)	17 (51.5)	14 (42.4)		
pT4a	28 (21.0)	8 (12.3)	20 (29.4)		12 (18.2)	1 (3.0)	11 (33.3)		
Nodal status				<.001				.011	.64
N0	88 (66.2)	56 (86.2)	32 (47.1)		41 (62.1)	26 (78.8)	15 (45.5)		
N1–3	45 (33.8)	9 (13.8)	36 (52.9)		25 (37.9)	7 (21.2)	18 (54.5)		
Lymphovascular invasion				<.001				.005	1.00
Absent	58 (43.6)	39 (69.6)	19 (31.7)		30 (45.5)	20 (69.0)	10 (31.3)		
Present	58 (43.6)	17 (30.4)	41 (68.3)		31 (47.0)	9 (31.0)	22 (68.7)		
Adjuvant chemotherapy				.022				.22	.17
Not administered	78 (58.6)	45 (69.2)	33 (49.3)		32 (48.5)	19 (57.6)	13 (39.4)		
Administered	54 (40.6)	20 (30.8)	34 (50.7)		34 (51.5)	14 (42.4)	20 (60.6)		
Status at last follow-up				<.001				<.001	.17
Alive	56 (42.1)	50 (76.9)	6 (8.8)		21 (31.8)	21 (63.6)	0 (0.0)		
Dead	77 (57.9)	15 (23.1)	62 (91.2)		45 (68.2)	12 (36.4)	33 (100)		

* P values based on two-sided Fisher's exact test.

† Except where noted

Figure 1. Performance of classifiers and individual clinicopathologic variables as assessed by standard-ROC analysis in the discovery and validation sets for predicting postcystectomy recurrence. GC had the highest AUC compared to single clinicopathologic variables. Its AUC increased when combined with IBCNC and CC. **Circles** and **whiskers** represent AUC and associated 95% confidence intervals, respectively. AUCs for variables are also listed under the respective sets. ROC = receiver-operating characteristic; AUC = area under ROC curve; GC = genomic classifier; IBCNC = postcystectomy recurrence nomogram from the International Bladder Cancer Nomogram Consortium; G-IBCNC = integrated genomic-IBCNC classifier; CC = "clinical-only" classifier; G-CC = integrated genomic-CC classifier.
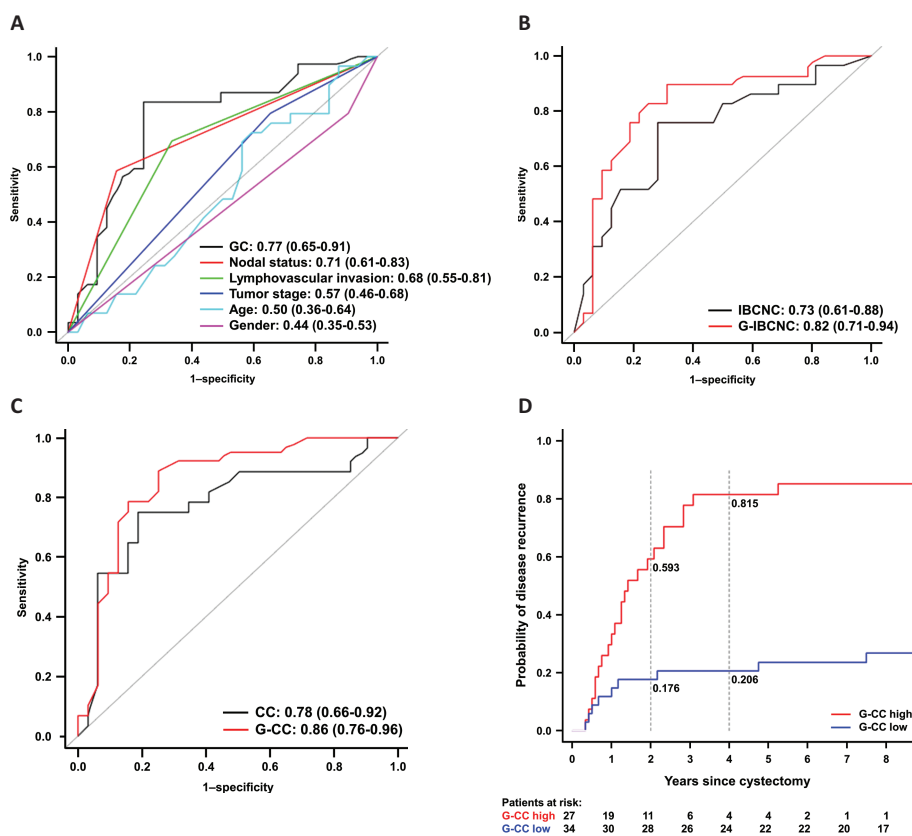
Figure 2. Performance of individual clinicopathologic variables and classifiers in the validation set for predicting cancer recurrence. **A)** Survival ROC curves show that GC outperforms individual clinicopathologic variables for predicting postcystectomy recurrence. In addition, **B)** G-IBCNC had higher AUC compared to IBCNC, and **C)** G-CC had higher AUC compared to CC by survival-ROC analysis. AUCs and associated 95% confidence intervals are shown at the bottom right of each ROC curve panel. **D)** Cumulative incidence plot for recurrence-free survival comparing patients with high versus low G-CC scores as determined by majority rule (cutoff = 0.5) indicate a statistically significantly elevated recurrence probability for patients with high G-CC scores (log-rank P < .001). Death from non-bladder-cancer causes was considered a competing risk. Probabilities of disease recurrence at 2 and 4 years postcystectomy are shown. All statistical tests were two-sided. ROC = receiver-operating characteristic; AUC = area under ROC curve; GC = genomic classifier; IBCNC = postcystectomy recurrence nomogram from the International Bladder Cancer Nomogram Consortium; G-IBCNC = integrated genomic-IBCNC classifier; CC = "clinical-only" classifier; G-CC = integrated genomic-CC classifier.

these markers into a GC, and this locked classifier assigned a score to each patient. The feature associated with *MECOM* was determined to be the most important variable (Supplementary Figure 3, available online). GC performance was compared with individual clinicopathologic variables, the IBCNC postoperative nomogram (8), and a clinical-only classifier (CC) that represented an optimized clinicopathologic prognostic model developed on the discovery set.

GC had an AUC of 0.88 (95% confidence interval [CI] = 0.81 to 0.93) in the discovery set (Figure 1). As GC was optimized in the discovery set, it could not be compared with individual clinicopathologic variables. However, we could assess the prognostic value of adding genomic information to clinical risk prediction models. When GC was added to IBCNC (G-IBCNC), the AUC increased from 0.73 to 0.89 (95% CI = 0.84 to 0.95). When GC was added to CC (G-CC), the AUC increased from 0.81 to 0.93 (95% CI = 0.88 to 0.97). This suggested that combined genomic-clinicopathologic classifiers could achieve superior prognostic performance than either alone.

Independent Validation of Genomic-Based Classifiers

Prognostic performance of the locked classifiers was then assessed (with bioinformaticians blinded to clinical variables) on an independent validation set of 66 UCB patients. Characteristics of patients in validation and discovery sets were comparable (Table 1).

Median age was 69.8 years (IQR = 63.1–74.3). Median follow-up was 10.8 years; 33 (50%) patients recurred, and 45 (68.2%) patients were dead at last follow-up. By univariate analysis, GC (P = .003), nodal status (P = .006) and lymphovascular invasion (P = .005) were prognostic for RFS, with GC having the highest hazard ratio (1.23 for every 10% score increment) (Table 2). GC performance as measured by standard ROC analysis was superior to single clinicopathologic variables (Figure 1). This was confirmed by survival ROC analysis where AUC for GC (0.77; 95% CI = 0.65 to 0.91) was higher than any individual clinicopathologic variable (Figure 2A).

Prognostic performance of IBCNC and CC were comparable (standard-ROC AUC = 0.74 and 0.77, respectively) with GC in the validation set. Again, performance of the combined genomic-clinicopathologic classifiers measured the highest of all models tested (Figure 1). Furthermore, AUCs by survival ROC analysis that consider time to recurrence showed marked boost in performance for combined models (IBCNC vs G-IBCNC, 0.73 vs 0.82; CC vs
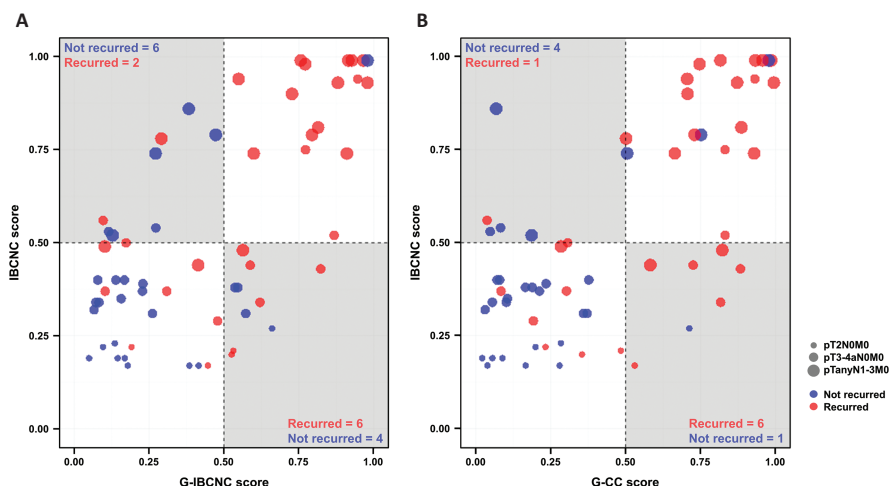
Figure 3. Reclassification of IBCNC score categories by genomic-clinicopathologic classifier scores for patients in the validation set. After categorizing based on their IBCNC scores, patients were reclassified based on their **A**) G-IBCNC and **B**) G-CC scores. Individual patients are represented as dots colored by recurrence event; sizes of dots represent pathological stage as indicated. **Gray quadrants** represent situations where the genomic-clinicopathologic classifier reclassifies patients compared

to IBCNC. Patients who did not recur (**blue dots**) in the top-left quadrant and patients who recurred (**red dots**) in the bottom-right quadrant are reclassified correctly by the genomic-clinicopathologic classifier. Of patients who were reclassified, a majority were done so correctly. IBCNC = postcystectomy recurrence nomogram from the International Bladder Cancer Nomogram Consortium; G-IBCNC = integrated genomic-IBCNC classifier; G-CC = integrated genomic-clinical classifier.

Table 2. Univariate associations of genomic and clinicopathologic features with risk of postcystectomy bladder cancer recurrence in the validation set*

	Relative risk of recurrence	
Predictor	**Hazard ratio (95% CI)**	**P**
GC	1.23 (1.07 to 1.42)	.003
Age <70 years	1.00 (0.99 to 1.01)	.72
Male sex	0.97 (0.89 to 1.06)	.46
Caucasian race	0.95 (0.85 to 1.05)	.29
Tumor stage [reference: pT2]		
pT1	1.02 (0.83 to 1.26)	.87
pT3	1.23 (0.50 to 3.05)	.66
pT4a	3.37 (1.27 to 8.93)	.015
Nodal status N1–3	1.10 (1.03 to 1.19)	.006
Lymphovascular invasion present	1.12 (1.03 to 1.20)	.005
Adjuvant chemotherapy administered	1.03 (0.96 to 1.11)	.35

* CI = confidence interval; GC = genomic classifier. HR estimated by Cox proportional hazards regression. All statistical tests were two-sided.

G-CC, 0.78 vs 0.86). Combined genomic-clinicopathologic classifiers had the highest specificity and sensitivity across the widest range of cutoffs (Figure 2, B and C). G-CC had the highest AUC among the combined genomic-clinicopathologic classifiers tested.

Multivariable analyses showed the independent prognostic significance of combined genomic-clinicopathologic classifiers compared with clinical models (Supplementary Table 2, available online). Decision curve analysis showed a higher overall net benefit for genomic-based classifiers, thereby highlighting their value as better tools for planning patient management compared to clinical-only risk models based on risk for recurrence (Supplementary Figure 4, available online). Discrimination plots confirmed that

Figure 4. Cumulative incidence plots for recurrence-free survival for node-negative patients in the validation set. Patients were stratified based on their **A)** CC and **B)** GC scores into high-risk and low-risk groups as determined by majority rule (cutoff = 0.5). Risk stratification based on GC scores was statistically significant ($P = .004$) while that based on CC scores showed a trend towards statistical significance ($P = .051$). Death from non-bladder-cancer causes was considered a competing risk. Probabilities of disease recurrence at 2 and 4 years postcystectomy are shown. P values were determined by the log-rank test and are two-sided. CC = "clinical-only" classifier; GC = genomic classifier.

while GC identified patients who recurred better than clinical models alone, the combined G-IBCNC and G-CC models were superior, with G-CC performing the best ($P = 5.55 \times 10^{-7}$) (Supplementary Figure 5, available online). G-CC was therefore considered the benchmark genomic-clinicopathologic classifier for further evaluation.

When survival-ROC AUCs were measured across a range of postcystectomy intervals, G-CC showed consistently superior performance compared with CC and GC alone, indicating that the former was most prognostic for RFS at any point in time following cystectomy (Supplementary Figure 6A, available online). Validation set patients were then categorized as high-risk (G-CC score ≥0.5) or low-risk (G-CC score <0.5). Accounting for competing risk, high-risk patients had elevated cumulative incidence of recurrence compared with low-risk patients (four-year probability: 81.5% vs 20.6%, respectively; $P < .001$) (Figure 2D). Patients were similarly risk-stratified by IBCNC and G-IBCNC scores, and categorization by the "clinical-only" IBCNC nomogram was compared with genomic-clinicopathologic classifiers (Figure 3). Addition of genomic features to the IBCNC nomogram (as G-IBCNC) reclassified 18 validation set patients into different predicted risk categories than those classified by IBCNC, of which 12 (66.7%) were reclassified correctly based on outcome. Similarly, G-CC reclassified 12 patients originally risk stratified by IBCNC, of which 10 (83.3%) were reclassified correctly.
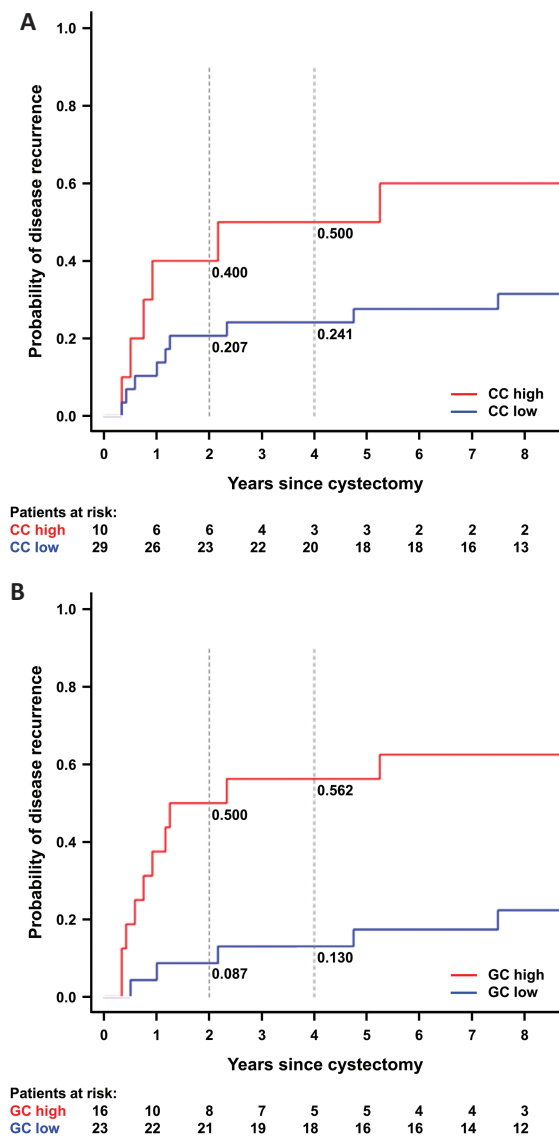
Nodal Status and Performance of Genomic-Based Classifier

When categorized by pathological stage, median GC scores were consistently higher in validation set patients who recurred (Supplementary Figure 7, available online). By multivariable analysis, after adjusting for demographic, clinicopathologic and treatment covariates, GC remained prognostic for recurrence ($P = .005$) (Table 3). In this analysis, a statistically significant interaction was noted between GC and nodal status ($P = .030$) that prompted further exploration of GC score distribution based on nodal stage. When categorized by nodal status, GC scores were able to better discriminate validation set patients based on recurrence status as evidenced by nonoverlapping 95% CIs of medians compared with CC (Supplementary Figure 8, available online) (29).
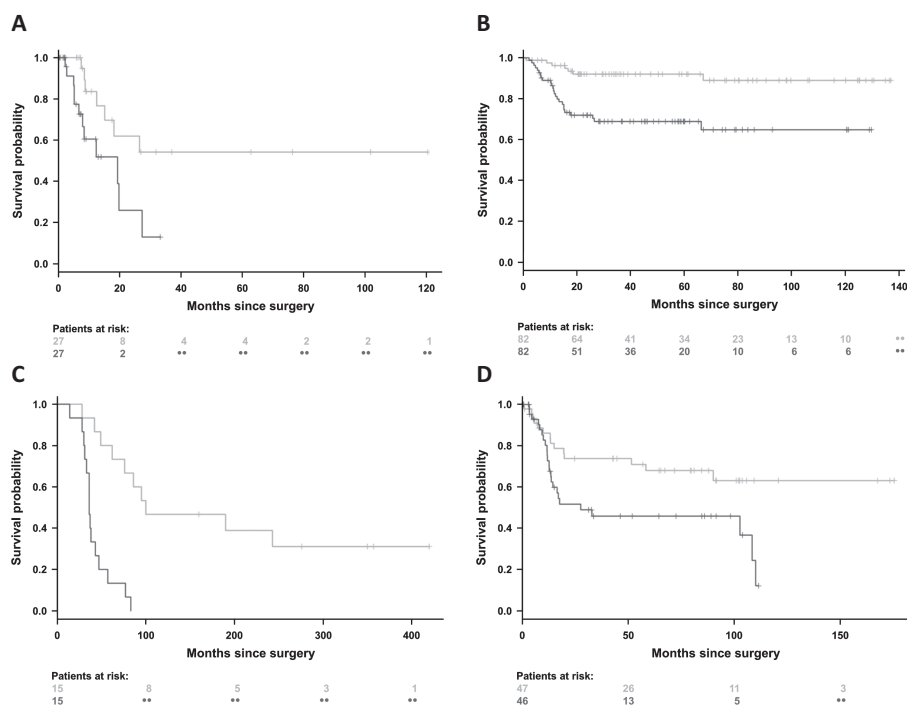
A subset analysis was then conducted on node-negative patients. These represent subjects who may not routinely receive adjuvant therapy. Assuming that higher-risk patients may gain more from therapy intensification, improved identification of such candidates using more accurate risk-prediction models could be beneficial. CC showed a trend towards significance in separating node-negative patients into risk groups ($P = .051$). However, GC statistically significantly stratified these patients based on recurrence (four-year probabilities: high 56.2% vs low 13%; $P = .004$) (Figure 4). When measured across time, AUCs for genomic-based classifiers were consistently higher compared with CC in node-negative patients (Supplementary Figure 6B, available online).

Analysis of Biological Processes and Prior Signatures

To analyze the biological relevance of features within GC, a network-based enrichment analysis of GO terms and biological pathways related to the markers and their 86 first-degree partners was performed

Figure 5. Kaplan-Meier survival plots showing independent external validation of GC performance. Bladder cancer patients from four external datasets including **A**) TCGA bladder urothelial carcinoma database (*P* = .016), **B**) NCBI–GEO GSE13507 (*P* < .001), **C**) NCBI–GEO GSE5287 (*P* < .001), and **D**) NCBI–GEO GSE31684 (*P* = .013) were stratified into low-risk (**green**) and high-risk (**red**) groups as determined by median split rule. Stratification was based on the prognostic index, which was calculated using all available markers related to the 15-feature GC. *P* values were determined by the log-rank test and are two-sided. GC = genomic classifier.

Table 3. Multivariable associations of genomic and clinicopathologic features with risk of postcystectomy bladder cancer recurrence in the validation set*

	Relative risk of recurrence	
Predictor and interaction terms	**Hazard ratio (95% CI)**	***P***
GC	1.42 (1.11 to 1.81)	.005
Age <70 years	0.90 (0.78 to 1.03)	.12
Male sex	0.00 (0.00 to 3.03)	.084
Caucasian race	0.36 (0.11 to 1.20)	.097
Tumor stage [reference: pT2]		
pT1	2.06 (0.15 to 27.73)	.59
pT3	1.82 (0.61 to 5.42)	.29
pT4a	1.83 (0.50 to 6.69)	.36
Nodal status N1–3	9.80 (1.50 to 64.04)	.017
Lymphovascular invasion present	2.74 (1.02 to 7.33)	.045
Adjuvant chemotherapy administered	0.94 (0.41 to 2.13)	.88
GC × nodal status †	0.03 (0.00 to 0.72)	.030
Sex × age †	1.12 (0.98 to 1.29)	.098

* CI = confidence interval; GC = genomic classifier. HR estimated by Cox proportional hazards regression. All statistical tests were two-sided.

† Interaction term

(Supplementary Figure 9, available online). Functional analysis revealed enrichment of pathways associated with cellular signaling including MAPK, WNT, and other cancer-associated processes. Additional GO clusters associated with cell movement and adhesion suggested roles in cell-cell interaction and tumor cell migration. This indicated that GC components likely reflect the pathobiology behind UCB development and progression beyond mere statistical associations.

Comparison with genes associated with UCB revealed that four markers within GC were identified in prior studies (Supplementary

Results, available online). The transcriptome-wide coverage of Human Exon arrays also allowed evaluation of previously reported prognostic signatures for muscle-invasive or node-positive UCB. Performances of seven genomic signatures were optimized in the discovery set and compared with GC (Supplementary Table 3) (13-15,21,22). As expected, nearly all prior signatures demonstrated high survival-ROC AUCs in the discovery set, as observed with GC. However, when these locked signatures were applied to the validation set with bioinformaticians being blinded to clinical variables,

the survival-ROC AUC for each model decreased, with GC having the best validated performance (Supplementary Figure 10, available online). A previously reported 61-feature panel for postcystectomy survival had the next-best performance in the validation set (AUC = 0.72; 95% CI = 0.60 to 0.87) (21).

External Validation of Genomic Classifier

Performance of the 15-feature GC was independently validated on 341 UCB patients from four external datasets sourced through TCGA and NCBI-GEO (13,21,30,31). When stratified based on the combined expression of GC markers, high-risk patients had statistically significantly poorer survival probabilities in all datasets ($P \leq .016$) (Figure 5). Concordance indices ranged from 0.65 to 0.80, and hazard ratios ranged from 2.23 to 7.57 across all available endpoints (Supplementary Table 4, available online).

Discussion

Patients with muscle-invasive or node-positive UCB at cystectomy are at higher risk for recurrence, although a substantial proportion remains recurrence-free after meticulous surgery and lymphadenectomy (2,32). Identification of candidates at highest risk for recurrence who may need adjuvant therapy is currently based on clinical criteria that may not reflect the entire biology of the disease (8). We hypothesized that an unbiased transcriptome-wide profiling approach of primary UCBs from clinically high-risk patients could be employed to accurately stratify the risk of postcystectomy recurrence. To our knowledge, this represents the largest effort to discover and validate a prognostic genomic signature for clinically high-risk UCB to date. The 15-feature GC surpassed the prognostic potential of standard clinical variables and previously reported genomic signatures for muscle-invasive UCB. Blinded and external validations confirmed the prognostic performance of genomic-based signatures. Such a tool can improve patient counseling after cystectomy and can better identify candidates who need more aggressive management.

Although patients with muscle-invasive UCB at cystectomy are considered to be at higher risk for recurrence clinically, most prior prognostic genomic profiling investigations have analyzed all UCB stages as part of their discovery effort, including non-muscle-invasive disease (13-15,21). Clinically high-risk patients in prior studies did not always receive consistent surgical management, and prognostic signatures were often generated towards non-disease-specific outcomes such as overall survival (Supplementary Table 3, available online). Further, prior efforts were limited to scarce frozen tumor specimens and employed low-density platforms that would only profile select protein-coding transcripts. The current study focused exclusively on identifying patients with muscle-invasive and/or node-positive UCB on final pathology who, based on expression profiles of their tumors, need intensified management to prevent recurrence. Patients were neoadjuvant chemotherapy-naïve, received consistent surgical management and had long follow-up. Performance of genomic signatures and clinical nomograms were measured against RFS, a highly disease-specific endpoint in this group of patients. Profiles were generated from FFPE tumors that represent an abundant and practical tissue source using technologies that reliably and reproducibly assess differential expression from archival specimens similar to unfixed tissues (33). The high-density profiling arrays in this investigation provide comprehensive whole-genome-scale coverage, including empirically supported and predicted transcribed sequences, enabling the discovery of previously unidentified events (34). This helped leverage the added value of noncoding transcripts that represent majority of the transcriptome, promote neoplastic transformation, and are potentially prognostic (35–37).

Addition of clinical information in the form of established (IBCNC) or novel (CC) nomograms to GC improved its performance, thereby suggesting that clinical and genomic variables provide independent and complementary prognostic information. Genomic-clinicopathologic classifiers had the highest net clinical benefit by decision curve analysis across a range of recurrence probabilities. When applied to node-negative patients, the subgroup where postcystectomy risk stratification is most critical (38), GC identified patients at risk for recurrence better than clinicopathologic metrics and remained statistically significant after adjusting for adjuvant chemotherapy administration. GC components include transcripts involved in cell proliferation and differentiation, apoptosis, cell-cycle and transcriptional regulation, and signal transduction—processes that are associated with UCB development and progression (39).

When benchmarked against previously reported gene signatures for clinically high-risk UCB, GC performance was superior when applied in a blinded manner on the validation set. This comparison was possible because of the transcriptome-wide profiling platform that allowed prior signatures to be modeled on our cohort. Of prior signatures' AUCs in the validation set, lower bounds of 95% CIs of 5/7 signatures were greater than 0.50, suggesting a statistically significant ability to predict recurrence beyond chance. This indicated that while some prior signatures were prognostic for clinically high-risk UCB, GC provides the highest relative performance that improved when combined with clinicopathologic metrics.

Study limitations include the inability to further evaluate GC because of the absence of public, clinically-annotated Human Exon array-profiled UCB datasets. However, its constituent markers could be mapped to other profiling platforms for assessment of performance. This exercise across four external datasets showed that GC could statistically significantly predict outcomes, thereby further validating its prognostic potential. Patients at elevated risk for recurrence may benefit from adjuvant therapy, although the efficacy of such therapy in patients with high GC or G-CC scores needs further investigation.

In conclusion, we document the discovery and validation of a 15-feature genomic classifier composed of biologically-relevant RNA sequences that can stratify patients with pathologically-confirmed muscle-invasive and/or node-positive UCB postcystectomy based on their risk for recurrence, especially when combined with clinicopathologic variables. Classifier performance was superior to clinical metrics and prior genomic signatures for such patients, and was validated in external datasets. This may be attributable to the use of a large cohort, clinically relevant endpoint, and high-density transcriptome-wide expression profiling approach. The standardized patient management and use of FFPE tissues for profiling also make this signature more clinically applicable. While additional analysis is warranted to better characterize the classifiers'

prognostic potential, our results suggest that the combination of these markers and clinicopathologic parameters may be prognostic for clinically high-risk UCB.

References

1. Jemal A, Bray F, Center MM, Ferlay J, Ward E, Forman D. Global cancer statistics. *CA Cancer J Clin*. 2011;61(2):69–90.
2. Stein JP, Lieskovsky G, Cote R, et al. Radical cystectomy in the treatment of invasive bladder cancer: long-term results in 1,054 patients. *J Clin Oncol*. 2001;19(3):666–675.
3. Shariat SF, Karakiewicz PI, Palapattu GS, et al. Outcomes of radical cystectomy for transitional cell carcinoma of the bladder: a contemporary series from the Bladder Cancer Research Consortium. *J Urol*. 2006;176(6):2414–2422.
4. Mitra AP, Quinn DI, Dorff TB, et al. Factors influencing post-recurrence survival in bladder cancer following radical cystectomy. *BJU Int*. 2012;109(6):846–854.
5. Rink M, Lee DJ, Kent M, et al. Predictors of cancer-specific mortality after disease recurrence following radical cystectomy. *BJU Int*. 2013;111(3b):E30–E36.
6. Leow JJ, Martin-Doyle W, Rajagopal PS, et al. Adjuvant chemotherapy for invasive bladder cancer: a 2013 updated systematic review and meta-analysis of randomized trials. *Eur Urol*. 2014;66(1):42–54.
7. Calabrò F, Sternberg CN. Neoadjuvant and adjuvant chemotherapy in muscle-invasive bladder cancer. *Eur Urol*. 2009;55(2):348–358.
8. *International Bladder Cancer Nomogram Consortium*. Postoperative nomogram predicting risk of recurrence after radical cystectomy for bladder cancer. *J Clin Oncol*. 2006;24(24):3967–3972.
9. Karakiewicz PI, Shariat SF, Palapattu GS, et al. Nomogram for predicting disease recurrence after radical cystectomy for transitional cell carcinoma of the bladder. *J Urol*. 2006;176(4):1354–1362.
10. Birkhahn M, Mitra AP, Cote RJ. Molecular markers for bladder cancer: the road to a multimarker approach. *Expert Rev Anticancer Ther*. 2007;7(12):1717–1727.
11. Stadler WM, Lerner SP, Groshen S, et al. Phase III study of molecularly targeted adjuvant therapy in locally advanced urothelial cancer of the bladder based on p53 status. *J Clin Oncol*. 2011;29(25):3443–3449.
12. Mitra AP, Bartsch CC, Cote RJ. Strategies for molecular expression profiling in bladder cancer. *Cancer Metastasis Rev*. 2009;28(3–4):317–326.
13. Riester M, Taylor JM, Feifer A, et al. Combination of a novel gene expression signature with a clinical nomogram improves the prediction of survival in high-risk bladder cancer. *Clin Cancer Res*. 2012;18(5):1323–1333.
14. Sanchez-Carbayo M, Socci ND, Lozano J, et al. Defining molecular profiles of poor outcome in patients with invasive bladder cancer using oligonucleotide microarrays. *J Clin Oncol*. 2006;24(5):778–789.
15. Blaveri E, Simko JP, Korkola JE, et al. Bladder cancer outcome and subtype classification by gene expression. *Clin Cancer Res*. 2005;11(11):4044–4055.
16. Mitra AP, Pagliarulo V, Yang D, et al. Generation of a concise gene panel for outcome prediction in urinary bladder cancer. *J Clin Oncol*. 2009;27(24):3929–3937.
17. Lindgren D, Frigyesi A, Gudjonsson S, et al. Combined gene expression and genomic profiling define two intrinsic molecular subtypes of urothelial carcinoma and gene signatures for molecular grading and outcome. *Cancer Res*. 2010;70(9):3463–3472.
18. Catto JW, Abbod MF, Wild PJ, et al. The application of artificial intelligence to microarray data: identification of a novel gene signature to identify bladder cancer progression. *Eur Urol*. 2010;57(3):398–406.
19. Mitra AP, Castelao JE, Hawes D, et al. Combination of molecular alterations and smoking intensity predicts bladder cancer outcome: a report from the Los Angeles Cancer Surveillance Program. *Cancer*. 2013;119(4):756–765.
20. Urinary bladder. In: Edge SB, Byrd DR, Compton CC, Fritz AG, Greene FL, Trotti A,eds. *AJCC Cancer Staging Manual*. 7th ed. New York, NY: Springer; 2010:497–505.
21. Kim WJ, Kim EJ, Kim SK, et al. Predictive value of progression-related gene classifier in primary non-muscle invasive bladder cancer. *Mol Cancer*. 2010;9:3.
22. Kim WJ, Kim SK, Jeong P, et al. A four-gene signature predicts disease progression in muscle invasive bladder cancer. *Mol Med*. 2011;17(5–6):478–485.
23. Fine JP, Gray RJ. A proportional hazards model for the subdistribution of a competing risk. *J Am Stat Assoc*. 1999;94(446):496–509.
24. Cui Q, Ma Y, Jaramillo M, et al. A map of human cancer signaling. *Mol Syst Biol*.2007;3:152.
25. Awan A, Bari H, Yan F, et al. Regulatory network motifs and hotspots of cancer genes in a mammalian cellular signalling network. *IET Syst Biol*. 2007;1(5):292–297.
26. Li L, Tibiche C, Fu C, et al. The human phosphotyrosine signaling network: evolution and hotspots of hijacking in cancer. *Genome Res*. 2012;22(7):1222–1230.
27. Newman RH, Hu J, Rho HS, et al. Construction of human activity-based phosphorylation networks. *Mol Syst Biol*. 2013;9:655.
28. Merico D, Isserlin R, Stueker O, Emili A, Bader GD. Enrichment map: a network-based method for gene-set enrichment visualization and interpretation. *PLoS One*.2010;5(11):e13984.
29. Chambers JM, Cleveland WS, Kleiner B, Tukey PA. *Graphical Methods for Data Analysis*. New Jersey, NJ: Wadsworth & Brooks/Cole Publishing Company; 1983.
30. *The Cancer Genome Atlas Research Network*. Comprehensive molecular characterization of urothelial bladder carcinoma. *Nature*. 2014;507(7492):315–322.
31. Als AB, Dyrskjøt L, von der Maase H, et al. Emmprin and survivin predict response and survival following cisplatin-containing chemotherapy in patients with advanced bladder cancer. *Clin Cancer Res*. 2007;13(15):4407–4414.
32. Logothetis CJ, Johnson DE, Chong C, et al. Adjuvant cyclophosphamide, doxorubicin, and cisplatin chemotherapy for bladder cancer: an update. *J Clin Oncol*. 1988;6(10):1590–1596.
33. Abdueva D, Wing M, Schaub B, Triche T, Davicioni E. Quantitative expression profiling in formalin-fixed paraffin-embedded samples by Affymetrix microarrays. *J Mol Diagn*. 2010;12(4):409–417.
34. Okoniewski MJ, Yates T, Dibben S, Miller CJ. An annotation infrastructure for the analysis and interpretation of Affymetrix exon array data. *Genome Biol*. 2007;8(5):R79.
35. Bernstein BE, Birney E, Dunham I, Green ED, Gunter C, Snyder M. An integrated encyclopedia of DNA elements in the human genome. *Nature*. 2012;489(7414):57–74.
36. Kapranov P, St Laurent G, Raz T, et al. The majority of total nuclear-encoded non-ribosomal RNA in a human cell is 'dark matter' un-annotated RNA. *BMC Biol*. 2010;8:149.
37. Mitra SA, Mitra AP, Triche TJ. A central role for long non-coding RNA in cancer. *Front Genet*. 2012;3:17.
38. Stockle M, Meyenburg W, Wellek S, et al. Adjuvant polychemotherapy of nonorgan-confined bladder cancer after radical cystectomy revisited: long-term results of a controlled prospective study and further clinical experience. *J Urol*. 1995;153(1):47–52.
39. Mitra AP, Cote RJ. Molecular pathogenesis and diagnostics of bladder cancer. *Annu Rev Pathol*. 2009;4:251–285

Notes

LLL, MG, NE, IAV, MA, CB, ZH, and TS are employees of GenomeDx Biosciences. TJT and ED own stock in GenomeDx Biosciences, which may offer the classifiers described in this study as patented commercial tests.

Affiliations of authors: Department of Pathology and Center for Personalized Medicine (APM, TJT) and Institute of Urology and Norris Comprehensive Cancer Center (SD), University of Southern California, Los Angeles, CA; GenomeDx Biosciences, Inc., Vancouver, BC (LLL, MG, NE, IAV, MA, CB, ZH, TS, TJT, ED); Department of Urology and the Stanford Cancer Institute, Stanford University, Stanford, CA (ECS); Department of Urologic Sciences, University of British Columbia, Vancouver, British Columbia, Canada (PCB).